JACS
JOURNAL OF THE AMERICAN CHEMICAL SOCIETY

Communication

pubs.acs.org/JACS

Preserving Both Anion and Cation Sublattice Features during a Nanocrystal Cation-Exchange Reaction: Synthesis of Metastable Wurtzite-Type CoS and MnS

Anna E. Powell,[‡] James M. Hodges,[‡] and Raymond E. Schaak*

Department of Chemistry and Materials Research Institute, The Pennsylvania State University, University Park, Pennsylvania 16802, United States

Supporting Information

ABSTRACT: The ability to selectively synthesize one particular polymorph in a solid-state system having multiple crystal structures with the same composition is important for accessing desired properties. Solution-mediated reactions, including anion and cation exchange, that chemically transform colloidal nanoparticles with pre-programmed structural features into targeted products have emerged as a powerful platform for predictably accessing metastable polymorphs. While nanocrystal ion-exchange reactions that retain anion sublattice features are well known, analogous reactions that preserve cation sublattice features are much less common, and guidelines for predictably targeting such sublattice features are not well established. Here, we report that both anion and cation sublattice features—hexagonal close-packed anions and tetrahedrally coordinated cations—can be preserved during cation exchange of roxbyite-type $Cu_{2-x}S$ nanocrystals to selectively produce wurtzite-type CoS and MnS. These polymorphs, which are metastable in bulk systems, form relative to other accessible structures having cubic close-packed anions and/or octahedrally coordinated cations. To facilitate these transformations, the scope of existing nanocrystal cation-exchange reactions was expanded to include 3d transition metal systems that previously have not been investigated in depth.

The crystal structure that a solid-state compound adopts is a primary determinant of its physical properties. Accordingly, predictable control of crystal structure is important during materials synthesis, especially for polymorphic systems where multiple crystal structures can exist. Many metal chalcogenide systems are well known to exhibit multiple polymorphs, where each phase can have distinct properties.[1] For example, the 2H (trigonal prismatic) and 1T (octahedral) polymorphs of MoS_2 are semiconducting and metallic, respectively, due to subtle differences in their stacking motifs and coordination environments.[2] Similarly, FeSe can crystallize in both PbO-type and NiAs-type structures, but only PbO-type FeSe is superconducting.[3] Since only one crystal structure in a metal chalcogenide system is thermodynamically favorable, predictably synthesizing less favorable polymorphs can be problematic and consequently remains a challenge in material synthesis.

Solution-mediated reactions that chemically transform colloidal nanoparticles (NPs) have emerged as a powerful platform for predictably accessing metastable polymorphs.[4] For example, anion- and cation-exchange reactions can topotactically transform NP templates, such as wurtzite-type ZnO or CdSe, into derivative products, such as wurtzite-type ZnS[5] or hexagonal Cu_2Se,[6] respectively. In bulk systems, such products are not the most stable polymorphs, but they are readily accessible via NP ion exchange due to the preservation of structural features. Generally, these reactions are facilitated by low reaction temperatures, which permit ion diffusion without disrupting sublattice structure, as well as chemical driving forces, such as solubility of the exchanging ions and complex formation.[7] Thus, the NP precursors can be considered as structural templates, offering a useful framework for predictably synthesizing a targeted metastable compound. Typically, when targeting metastable crystal structures using cation-exchange methods, the rigid anion sublattice of the nanocrystal template can be retained during the transformation.[8] Preservation of cation sublattice features is less common,[9] and consequently less understood, although insights into these processes could improve design guidelines for rationally targeting synthetically challenging polymorphs.

Accordingly, here we report that both anion and cation sublattice features can be preserved during cation-exchange reactions of roxbyite-type $Cu_{2-x}S$ NPs to produce wurtzite-type CoS and MnS products, which are metastable in bulk systems. Such insights offer useful guidelines for predictably targeting structural features in nanocrystalline metal chalcogenides. To achieve structural templating in these systems, the scope of existing NP cation-exchange reactions was significantly expanded to include 3d transition metal systems that previously have not been investigated in depth, thereby opening the door to cation-exchange reactions in new classes of materials. This is also important, because a majority of NP cation-exchange chemistry focuses on reactions involving the late transition metal and post-transition metal systems Ag^+, Cu^+, Cd^{2+}, Pb^{2+}, and Zn^{2+}.[7a]

The formation of wurtzite-type CoS and MnS by cation exchange of roxbyite-type $Cu_{2-x}S$ serves as an instructive system for studying the simultaneous retention of anion and cation sublattice features during NP ion-exchange reactions (Figure 1). Roxbyite-type $Cu_{2-x}S$ is typically described as having a distorted hexagonal close-packed (hcp) framework of S^{2-} anions with Cu^+ cations occupying a variety of distorted trigonal and tetrahedral

Received: October 10, 2015
Published: December 22, 2015

DOI: 10.1021/jacs.5b10624
J. Am. Chem. Soc. 2016, 138, 471−474

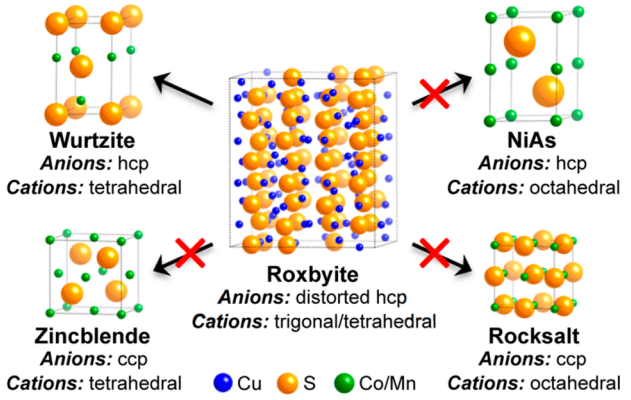

Figure 1. Selective transformation of roxbyite $Cu_{2-x}S$ into wurtzite CoS and MnS relative to the zincblende, NiAs, and rocksalt polymorphs, which all are structurally related and also well known to form for CoS (NiAs) and MnS (rocksalt, zincblende) using pathways that do not involve nanoparticle ion exchange. Arrows covered by a red × indicate transformations that are not observed; here, only the transformation of roxbyite to wurtzite is observed. Unit cells are outlined in black, and characteristic anion stacking sequences (hcp = hexagonal close-packed, ccp = cubic close-packed) and cation coordination environments (octahedral, tetrahedral) are indicated for each structure. The observed selective roxbyite-to-wurtzite transformation suggests simultaneous conservation of hcp anion stacking sequence and tetrahedral cation coordination environment.

coordination environments.[10] Wurtzite-type CoS and MnS, which are both metastable phases in bulk systems, have tetrahedrally coordinated metal cations in a hcp array of sulfide anions. In contrast, their most stable polymorphs, NiAs-type CoS and rocksalt-type MnS, both contain octahedrally coordinated metal cations, but the sulfide anions in NiAs-type CoS are hcp while in rocksalt-type MnS the sulfide anions are cubic close-packed (ccp). Wurtzite-type CoS has been claimed to form as films through chemical bath deposition methods,[11] but it has not been accessed as powders in isolatable quantities. Wurtzite-type MnS has been synthesized through a variety of approaches including colloidal,[12] solvothermal,[13] microwave irradiation,[14] and chemical vapor deposition[15] methods. As described in detail below, the exclusive formation of wurtzite-type CoS and MnS via cation exchange of roxbyite-type $Cu_{2-x}S$, which all share common structural features, suggests that both anion and cation sublattice features are preserved during the process.

Roxbyite-type $Cu_{2-x}S$ was synthesized by heating $Cu(acac)_2$ and sulfur in oleylamine to 200° for 1 h;[16] see the Supporting Information for complete experimental details. The powder XRD pattern for the NPs (Figure S1) matches well with that expected for roxbyite-type $Cu_{2-x}S$. Figures 2a and S2 show transmission electron microscopy (TEM) images, which reveal uniform circular platelets having average thicknesses and diameters of ~6 × 16 nm, respectively. The selected area electron diffraction (SAED) pattern shown in Figure S2 confirms that the NPs consist of roxbyite-type $Cu_{2-x}S$.

Copper sulfides have been used as NP templates for cation exchange to form post-transition metal chalcogenide products such as CdS, PbS, and ZnS,[4c,17] but no analogous cation-exchange reactions involving 3d transition metals, including Co^{2+} and Mn^{2+}, have been reported beyond the minimal incorporation of dopants into oxide and chalcogenide hosts.[18] We find that cation exchange of $Cu_{2-x}S$ nanocrystals using Co^{2+} and Mn^{2+} can be achieved by reacting the $Cu_{2-x}S$ templates with the appropriate metal precursor at elevated temperatures in the presence of tri-*n*-

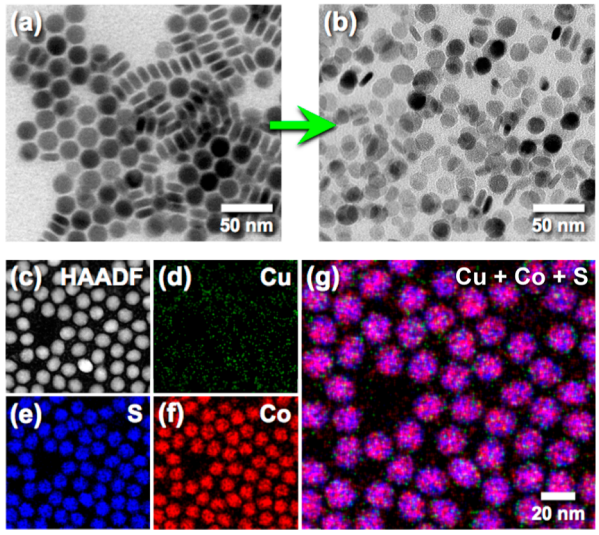

Figure 2. Representative TEM images of (a) roxbyite-type $Cu_{2-x}S$ and (b) wurtzite-type CoS particles, showing retention of circular platelet morphology during cation exchange. (c) HAADF STEM image and (d–f) corresponding STEM-EDS element maps for Cu, Co, and S, with an overlay in (g), confirming the composition of the exchange product.

octylphosphine (TOP), similar to a protocol used to facilitate the transformation of Cu_xSe into ZnSe.[6,7b] Accordingly, upon reaction of the $Cu_{2-x}S$ NPs in TOP with a cobalt–oleylamine complex in toluene at 100 °C for 10 min, wurtzite-type CoS forms, as shown by the powder XRD data in Figure 3. The refined

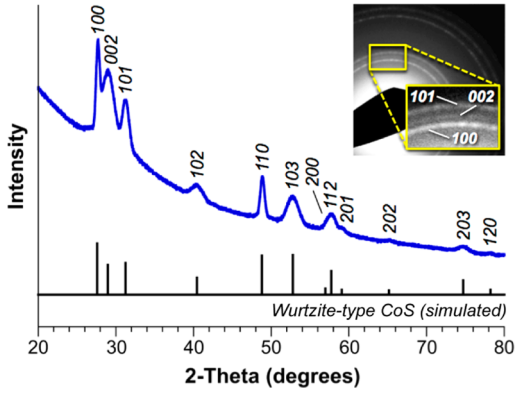

Figure 3. Indexed powder XRD pattern of wurtzite-type CoS platelets: top, experimental; bottom, simulated. Inset: Indexed SAED pattern corresponding to the wurtzite-type CoS particles, emphasizing the characteristic (100), (002), and (101) reflections.

hexagonal lattice constants for the wurtzite-type CoS product are a = 3.730(2) Å and c = 6.162(2) Å, smaller than for the comparable wurtzite-type compounds ZnS (a = 3.8227 Å, c = 6.2607 Å) and MnS (a = 3.9792 Å, c = 6.4469 Å), as expected based on known ionic radii values.[19]

The TEM images in Figures 2b and S3 show that the circular platelet morphology of the roxbyite $Cu_{2-x}S$ precursor is retained, as are the average dimensions of ~6 × 16 nm, upon cation exchange. A high-resolution TEM (HRTEM) image of the side of a platelet (Figure 4a) reveals lattice spacings of 3.0 Å, corresponding to the (002) plane of wurtzite-type CoS. A top-view HRTEM image of the platelet (Figure 4b) shows lattice spacings 2.9 and 3.2 Å, corresponding to the (101) and (100) planes. Scherrer analysis of the (100) and (002) peaks in the

DOI: 10.1021/jacs.5b10624
J. Am. Chem. Soc. 2016, 138, 471–474

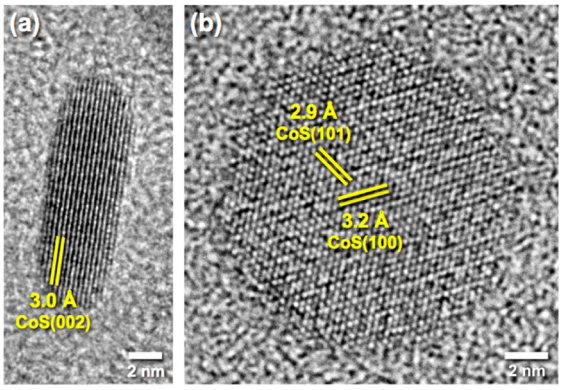

Figure 4. HRTEM images showing (a) side and (b) top views of a wurtzite-type CoS particle.

XRD pattern in Figure 3 indicates grain sizes of 13 and 5 nm, respectively, in agreement with both the HRTEM lattice fringes and the average particle dimensions observed by TEM. In addition, Scherrer analysis of the (101) plane, which runs diagonally through the particles, revealed an intermediate thickness of 8 nm, as expected based on the platelet morphology and the corresponding relative coherence lengths of the (100), (002), and (101) planes (Figure S4). The SAED pattern in the Figure 3 inset further confirms that the NPs are wurtzite-type CoS. Energy-dispersive X-ray spectroscopy (EDS) data (Figure S5) confirm the expected ~1:1 Co:S ratio, as well as the presence of only small amounts (~1%) of residual Cu, in the CoS product. A scanning transmission electron microscopy (STEM) high-angle annular dark field (HAADF) image, coupled with STEM-EDS element maps for the CoS NPs (Figure 2c–g), confirms the expected co-localization of Co and S, as well as the presence of only small amounts of residual Cu. While not the primary focus of this work, the wurtzite-type CoS NPs can be further cation-exchanged to re-generate roxbyite-type $Cu_{2-x}S$ (Figure S6). This additional cation-exchange process again maintains morphology, although there is some loss of crystallinity.

Formation of wurtzite-type CoS upon cation exchange of roxbyite-type $Cu_{2-x}S$ is interesting and important because NiAs-type CoS is the most stable polymorph and wurtzite-type CoS, as a bulk solid, is metastable. It is well known that anion sublattice structure often can be retained upon both cation- and anion-exchange reactions, as mentioned previously. However, both wurtzite-type CoS and NiAs-type CoS have a hcp anion framework. While roxbyite-type $Cu_{2-x}S$ has an anion framework that is considered to be a distorted variant of hcp, formation of wurtzite-type CoS rather than the more stable NiAs polymorph cannot be driven by preservation of the anion framework alone, since both are hcp. Figure 5a shows a [010] projection of the roxbyite crystal structure next to crystallographically equivalent projections of the wurtzite and NiAs crystal structures, as well as a diagram depicting the vertical registries of the tetrahedral and octahedral holes relative to the close-packed layers in Figure 5b. The cations in roxbyite-type $Cu_{2-x}S$ adopt a variety of distorted trigonal and tetrahedral sites in the distorted hcp array of sulfide anions, but importantly, the octahedral holes are vacant. Roxbyite-type $Cu_{2-x}S$ also contains Cu vacancies in nominally tetrahedral sites that could serve as channels for facilitating cation exchange (Figure 5c). Indeed, such copper sulfides are known to have high cation mobilities,[17] and Cu vacancies in $Cu_{2-x}Se$ nanocrystals have been shown to promote cation exchange.[20]

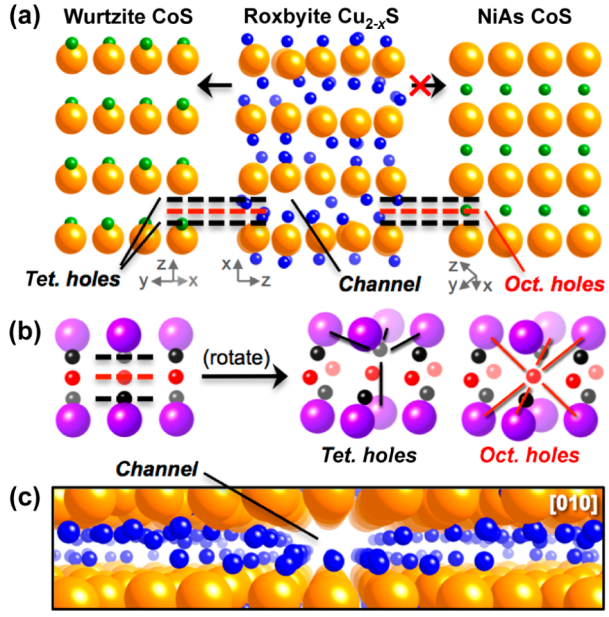

Figure 5. (a) Crystallographically related projections of the wurtzite, roxbyite, and NiAs structures, emphasizing the vertical registries of the tetrahedral and octahedral holes (black and red dashed lines, respectively), as well as the cation vacancies in roxbyite that create open channels. (b) Generic AB hcp layer sequence (purple), aligned analogous to the wurtzite and NiAs structures in (a), showing the vertical registries of the tetrahedral (black) and octahedral (red) holes, as well as the tetrahedral and octahedral coordination environments. (c) Enlarged [010] projection of a single layer of roxbyite, highlighting open channels that could aid in cation diffusion within the plane containing the tetrahedral holes.

Comparing the structures in Figure 5 thus suggests that wurtzite-type CoS may form because cation exchange occurs through a pathway that maintains the nominal tetrahedral coordination environment of the roxbyite-type $Cu_{2-x}S$ template (the coordination environment in which the vacancies lie), disfavoring filling of the octahedral holes as would be required to form NiAs-type CoS. Other factors could also contribute to the observed anion and cation sublattice retention. For example, the small amount of residual Cu after exchange of $Cu_{2-x}S$ with Co^{2+} could help to stabilize the wurtzite structure, as could microstructural contributions such as strain. Additionally, the pseudohexagonal lattice constants for the distorted hcp S^{2-} sublattice in the roxbyite $Cu_{2-x}S$ structure have average values of a = 3.87 Å and c = 6.71 Å, corresponding to a c/a ratio of 1.73. The c/a ratio of roxbyite-type $Cu_{2-x}S$ is much closer to that of wurtzite-type CoS (c/a = 1.65) than to that of NiAs-type CoS (c/a = 1.53); this also may contribute, in part, to the preferential formation of wurtzite-type CoS after cation exchange.

Cation exchange of roxbyite-type $Cu_{2-x}S$ with Mn^{2+} was also studied under similar reaction conditions as described for cation exchange with Co^{2+} (see Supporting Information for complete experimental details). Indeed, as shown in Figure 6, the product is wurtzite-type MnS. The XRD pattern in Figure S7 matches well with that expected for wurtzite-type MnS (a = 3.99 Å, c = 6.43 Å), with anisotropic peak broadening consistent with the platelet morphology defined by the $Cu_{2-x}S$ precursor. The TEM image in Figure 6a confirms the formation of particles having a circular platelet morphology matching that of the $Cu_{2-x}S$ precursor, and the corresponding SAED pattern in Figure 6b shows evidence of significant preferred orientation, along with

DOI: 10.1021/jacs.5b10624
J. Am. Chem. Soc. 2016, 138, 471–474

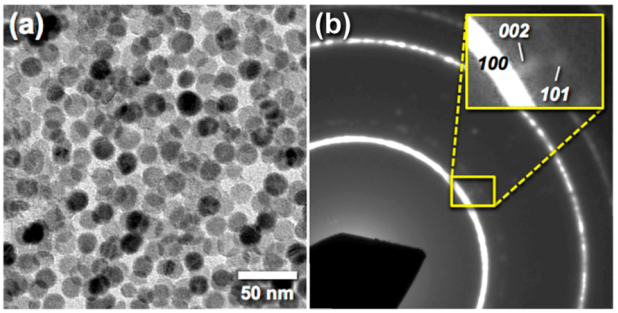

Figure 6. Representative (a) TEM image and (b) SAED pattern of wurtzite-type MnS particles.

diffraction spots diagnostic of wurtzite-type MnS. Figure S7, which shows a HAADF-STEM image and the corresponding STEM-EDS maps, indicates that Mn and S are co-localized on the particles, as expected. The EDS spectrum in Figure S7 indicates that the MnS product contains ~10% residual Cu, more than that in CoS.

Formation of wurtzite-type MnS, with tetrahedral metal cation coordination in a hcp array of sulfide anions, is particularly significant, because MnS has three polymorphs that can be accessed as colloidal NPs—rocksalt, wurtzite, and zincblende.[21] Rocksalt- and zincblende-type MnS have a ccp anion sublattice, while wurtzite-type MnS has a hcp anion sublattice. Zincblende- and wurtzite-type MnS have tetrahedral metal cation coordination while rocksalt-type MnS has octahedral metal cation coordination. Selectively and exclusively forming the wurtzite polymorph of MnS thus also suggests that both anion (hcp vs ccp) and cation (tetrahedral vs octahedral) sublattice features from roxbyite-type $Cu_{2-x}S$ were retained during the cation-exchange process.

In summary, we have extended colloidal nanocrystal cation-exchange reactions to 3d transition metal systems in order to study the transformation of roxbyite $Cu_{2-x}S$ into wurtzite CoS and MnS, which are metastable as bulk compounds. Our observations support the hypothesis that both anion *and* cation sublattice features can be retained during nanocrystal cation-exchange reactions, although more comprehensive studies are needed to fully investigate all key factors that may play contributing roles. In addition to expanding the scope of cation-exchange reactions beyond the late transition metal and post-transition metal systems studied previously, these results provide useful guidelines for predictably targeting desired structural features in nanocrystalline metal chalcogenides and for selectively accessing one of multiple phases in polymorphic solid-state systems.

■ ASSOCIATED CONTENT

Supporting Information

The Supporting Information is available free of charge on the ACS Publications website at DOI: 10.1021/jacs.5b10624.

Complete experimental details and additional characterization data, including Figures S1−S7 (PDF)

■ AUTHOR INFORMATION

Corresponding Author

*res20@psu.edu

Author Contributions

‡A.E.P. and J.M.H. contributed equally.

Notes

The authors declare no competing financial interest.

■ ACKNOWLEDGMENTS

This work was supported by the U.S. National Science Foundation (grant DMR-1305564). TEM imaging was performed in the Penn State Microscopy and Cytometry facility, and HRTEM imaging at the Materials Characterization Lab of the Penn State Materials Research Institute. The authors thank Profs. Kate Plass and Bryce Sadtler for helpful discussions.

■ REFERENCES

(1) (a) Rao, C. N. R.; Pisharody, K. P. R. *Prog. Solid State Chem.* **1976**, *10*, 207. (b) Corliss, L.; Elliott, N.; Hastings, J. *Phys. Rev.* **1956**, *104*, 924. (c) Scanlon, D. O.; et al. *Nat. Mater.* **2013**, *12*, 798. (d) Lourembam, J.; Srivastava, A.; La-o-vorakiat, C.; Rotella, H.; Venkatesan, T.; Chia, E. E. M. *Sci. Rep.* **2015**, *5*, 9182. (e) Sines, I. T.; Misra, R.; Schiffer, P.; Schaak, R. E. *Angew. Chem., Int. Ed.* **2010**, *49*, 4638.

(2) (a) Huang, X.; Zeng, Z.; Zhang, H. *Chem. Soc. Rev.* **2013**, *42*, 1934. (b) Lin, Y.-C.; Dumcenco, D. O.; Huang, Y.-S.; Suenaga, K. *Nat. Nanotechnol.* **2014**, *9*, 391.

(3) (a) Hsu, F.-C.; et al. *Proc. Natl. Acad. Sci. U.S.A.* **2008**, *105*, 14262. (b) McQueen, T. M.; et al. *Phys. Rev. B* **2009**, *79*, 014522.

(4) (a) Li, H.; Brescia, R.; Povia, M.; Prato, M.; Bertoni, G.; Manna, L.; Moreels, I. *J. Am. Chem. Soc.* **2013**, *135*, 12270. (b) Dawood, F.; Schaak, R. E. *J. Am. Chem. Soc.* **2009**, *131*, 424. (c) Luther, J. M.; Zheng, H.; Sadtler, B.; Alivisatos, A. P. *J. Am. Chem. Soc.* **2009**, *131*, 16851.

(5) Park, J.; Zheng, H.; Jun, Y.; Alivisatos, A. P. *J. Am. Chem. Soc.* **2009**, *131*, 13943.

(6) Li, H.; Zanella, M.; Genovese, A.; Povia, M.; Falqui, A.; Giannini, C.; Manna, L. *Nano Lett.* **2011**, *11*, 4964.

(7) (a) Rivest, J. B.; Jain, P. K. *Chem. Soc. Rev.* **2013**, *42*, 89. (b) Beberwyck, B. J.; Alivisatos, A. P. *J. Am. Chem. Soc.* **2012**, *134*, 19977.

(8) Jain, P. K.; Amirav, L.; Aloni, S.; Alivisatos, A. P. *J. Am. Chem. Soc.* **2010**, *132*, 9997.

(9) Hodges, J. M.; Kletetschka, K.; Fenton, J. L.; Read, C. G.; Schaak, R. E. *Angew. Chem., Int. Ed.* **2015**, *54*, 8669.

(10) Mumme, W. G.; Gable, R. W.; Petricek, V. *Can. Mineral.* **2012**, *50*, 423.

(11) Mane, S. T.; Kamble, S. S.; Deshmukh, L. P. *Mater. Lett.* **2011**, *65*, 2639.

(12) Joo, J.; Na, H. B.; Yu, T.; Yu, J. H.; Kim, Y. W.; Wu, F.; Zhang, J. Z.; Hyeon, T. *J. Am. Chem. Soc.* **2003**, *125*, 11100.

(13) Lu, J.; Qi, P.; Peng, Y.; Meng, Z.; Yang, Z.; Yu, W.; Qian, Y. *Chem. Mater.* **2001**, *13*, 2169.

(14) Wang, S.; Li, K.; Zhai, R.; Wang, H.; Hou, Y.; Yan, H. *Mater. Chem. Phys.* **2005**, *91*, 298.

(15) Beltran-Huarac, J.; Resto, O.; Carpena-Nuñez, J.; Jadwisienczak, W. M.; Fonseca, L. F.; Weiner, B. R.; Morell, G. *ACS Appl. Mater. Interfaces* **2014**, *6*, 1180.

(16) Lotfipour, M.; Machani, T.; Rossi, D. P.; Plass, K. E. *Chem. Mater.* **2011**, *23*, 3032.

(17) Ha, D.-H.; Caldwell, A. H.; Ward, M. J.; Honrao, S.; Mathew, K.; Hovden, R.; Koker, M. K. A.; Muller, D. A.; Hennig, R. G.; Robinson, R. D. *Nano Lett.* **2014**, *14*, 7090.

(18) (a) Sytnyk, M.; et al. *Nano Lett.* **2013**, *13*, 586. (b) Eilers, J.; Groeneveld, E.; de Mello Donegá, C.; Meijerink, A. *J. Phys. Chem. Lett.* **2012**, *3*, 1663.

(19) Shannon, R. D.; Prewitt, C. T. *Acta Crystallogr., Sect. B* **1969**, *25*, 925.

(20) Lesnyak, V.; Brescia, R.; Messina, G. C.; Manna, L. *J. Am. Chem. Soc.* **2015**, *137*, 9315.

(21) Yang, X.; Wang, Y.; Wang, K.; Sui, Y.; Zhang, M.; Li, B.; Ma, Y.; Liu, B.; Zou, G.; Zou, B. *J. Phys. Chem. C* **2012**, *116*, 3292.

DOI: 10.1021/jacs.5b10624
J. Am. Chem. Soc. 2016, 138, 471−474